

Automatic crosswell tomography by differential semblance optimization

René-Edouard Plessix, Fons ten Kroode and Wim Mulder, *Shell Int'l E&P*

Summary

In this paper, a method for automatic tomography based on semblance and differential semblance is presented. The method determines the background velocity from the first arrivals. A semblance panel is built by back-propagating all the seismic data traces towards zero time. If the background velocity is close to the true one, all the first-arrival-transmitted waves are lined up at zero time and the back-propagated traces are almost identical. The velocity model is then updated either by maximizing the norm of the stack of all the back-propagated traces (semblance optimization) or by minimizing the norm of the difference between two adjacent traces (differential semblance optimization).

Introduction

We present an automatic tomographic algorithm that inverts crosswell seismic data for the (background) velocity, based on semblance or differential semblance [5]. The main difficulty in tomographic inversion is caused by the strong non-linear dependence of the direct-arrival wavefront on the velocity. Therefore, the least-squares approach namely the minimization of the difference between observed and synthetic crosswell data leads to an oscillatory cost function. The search for the global solution requires the use of a stochastic optimization algorithm, which is very time consuming. To obtain a faster algorithm, we must find a cost function with a sufficiently large basin of attraction to allow for the use of a gradient optimization.

The common approach to recover the velocity is tomography based on picked first-arrival travel-times. The advantage of working with the travel-times is their linear dependence on the slowness (inverse of the velocity) along the ray-paths. However, for practical applications the task of picking the first arrivals can be overwhelming.

An attractive method to automate tomography consists of working on semblance panels. Given a velocity model, the travel-times between the sources and receivers are used to back-propagate the seismic traces towards zero time. The set of all the back-propagated traces is called the semblance panel. Assuming that the first-arrival transmitted waves are the most energetic, all the back-propagated traces are (almost) lined-up and identical if the velocity model is the true one. The measure of the differences in the semblance panel then gives a measure of the quality of the velocity model. Therefore, the velocity model can be updated by maximizing the stack of all the traces in the semblance panel (semblance optimization) or by minimizing the

difference between adjacent traces (differential semblance optimization). It has been numerically shown that the differential semblance cost function can be optimized by a gradient method thanks to a fairly large basin of attraction [1], [5], [6].

In this paper, the method is briefly described using the ray or high-frequency approximation. Also the constraints added to the optimization to improve the inversion results are explained. Then results on synthetic and real data are given. For all these examples, the cost functions are optimized by a quasi-Newton algorithm and an exact gradient computation [4].

Method

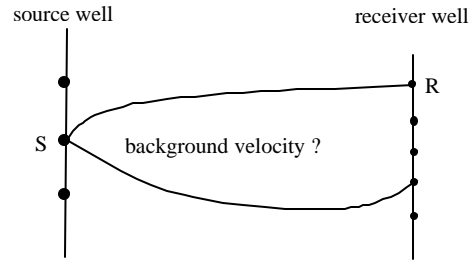


Figure 1: survey geometry

The well geometry studied here corresponds to two vertical wells (see Figure 1). With the high-frequency approximation and assuming that the first-arrival-transmitted waves are the most energetic, the seismic crosswell data can be modeled by

$$u[\sigma](\mathbf{x}_S, \mathbf{x}_R)(t) = a[\sigma](\mathbf{x}_S, \mathbf{x}_R) f(t - \tau[\sigma](\mathbf{x}_S, \mathbf{x}_R)),$$

where σ is the slowness, \mathbf{x}_S and \mathbf{x}_R are the source and receiver position, respectively, τ is the travel-time, a the amplitude, and f the source wavelet.

In this way, the problem consists of finding σ_{true} such that

$$d(\mathbf{x}_S, \mathbf{x}_R) \approx u[\sigma_{\text{true}}](\mathbf{x}_S, \mathbf{x}_R),$$

where d is the set of observed data.

The semblance trace, s , is the back-propagated seismic trace:

$$s[\sigma](\mathbf{x}_S, \mathbf{x}_R)(t) = d(\mathbf{x}_S, \mathbf{x}_R)(t + \tau[\sigma](\mathbf{x}_S, \mathbf{x}_R)) / a[\sigma](\mathbf{x}_S, \mathbf{x}_R).$$

Under these assumptions, we have for any source and receiver position

Automatic crosswell tomography

$$s[\sigma_{\text{true}}](\mathbf{x}_S, \mathbf{x}_R)(t) \approx f(t),$$

which demonstrates that the first-arrival-transmitted waves must be lined up in the semblance panel.

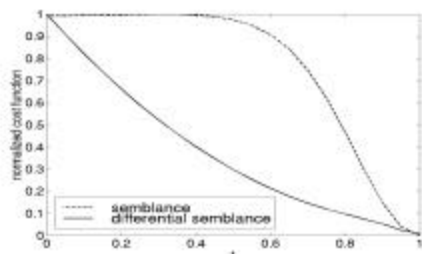


Figure 2: slice of the semblance and differential semblance cost function. Using the synthetic example, the evolution of the cost function has been plotted when the background velocity linearly varies from 3800 m/s (for $t=0$) to the true one (for $t=1$).

To measure this lining-up, we can use the stack of all the semblance traces. This leads to semblance optimization. The optimal velocity model is obtained by maximizing the semblance cost function

$$S(\sigma) = \int dt \left| \int_{\mathbf{x}_S} d\mathbf{x}_S \int_{\mathbf{x}_R} d\mathbf{x}_R s[\sigma](\mathbf{x}_S, \mathbf{x}_R)(t) \right|^2.$$

In Figure 2, a slice of the semblance cost function is drawn. The basin of attraction is fairly large. However, when the velocity model is far from the true one, this cost function is almost flat and therefore carries very little information on the velocity model. In fact, in this area the stack is almost completely destructive.

Symes has proposed the use of a *differential* approach to overcome this difficulty [5], [6]. The measure of the lining-up of the first-arrivals in the semblance panel is computed by the norm of the difference between adjacent traces. This leads to the differential semblance optimization: the optimal velocity model is found by minimizing the differential semblance cost function

$$DS(\sigma) = \int_{\mathbf{x}_S} d\mathbf{x}_S \int_{\mathbf{x}_R} d\mathbf{x}_R \int dt \left| \frac{\partial s[\sigma](\mathbf{x}_S, \mathbf{x}_R)(t)}{\partial \mathbf{x}_S} \right|^2.$$

(Here \mathbf{x}_S is the semblance parameter, however other semblance parameters can be used, for instance \mathbf{x}_R .)

In Figure 2, a slice of the differential cost function is drawn. The basin of attraction is larger than that of the semblance cost function thanks to the local comparison. This function will therefore allow us to start with a relatively poor first guess. For a mathematical study of differential semblance, we refer to Symes' papers.

Both the semblance and differential semblance cost function try to line up the first-arrivals. However it can happen that this lining up occurs not only at zero time. To prevent this, a regularization term of the following form is added:

$$R(\sigma) = \int_{\mathbf{x}_S} d\mathbf{x}_S \int_{\mathbf{x}_R} d\mathbf{x}_R \int dt |w(t) s[\sigma](\mathbf{x}_S, \mathbf{x}_R)(t)|^2$$

where w is a weight function ($w(t)=t^2$ for example).

Another difficulty is that the transmitted waves in crosswell seismic data carry little information on the lateral variation [2]. To improve the recovery of these lateral variations, we use difference of the slowness with respect to the sonic logs at the well positions as an additional penalty term in the cost function.

Before describing the examples, it is important to recall that this approach assumes that the first-arrival transmitted wave is the most energetic in the data trace. Unfortunately part of the data does not satisfy this assumption, for instance in the presence of channel waves. To process real data, the traces where multi-valuedness occurs are blanked.

A synthetic example

For the velocity model shown in Figure 3, we have computed synthetic data for 64 shots and 64 receivers. One shot panel is plotted in Figure 4.

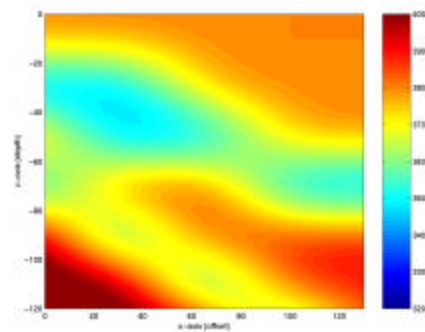


Figure 3: True velocity of the synthetic example

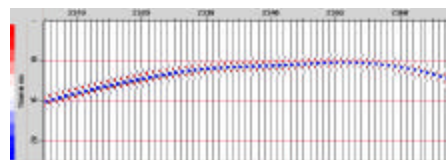


Figure 4: shot panel (the horizontal axis represents the receivers and the vertical axis the time).

Automatic crosswell tomography

During the optimization of the differential cost function, the velocity at the well positions is known. The first guess is deduced from the well velocity by interpolation and shown in Figure 5.

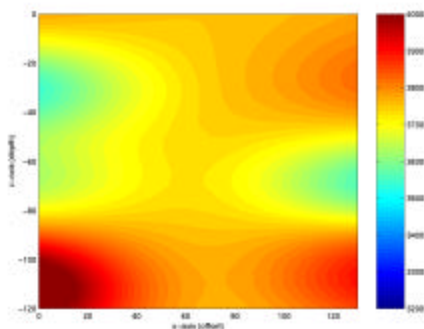


Figure 5: initial guess deduced from the velocity at the well positions.

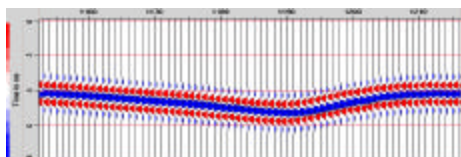


Figure 6: initial semblance panel (computed for the initial guess).

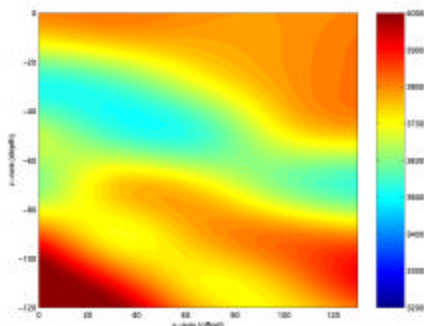


Figure 7: optimal velocity model

After minimization of the differential semblance cost function, the error between the optimal velocity, shown in Figure 7, and the true one, Figure 3, is less than 3%. The first-arrivals are lined up in the final semblance panel, Figure 8, demonstrating that the optimal velocity correctly interprets the data.

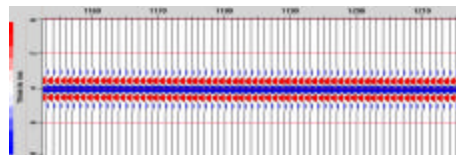


Figure 8: optimal semblance panel.

Real example: Mc Elroy data set

We have tried to invert the crosswell data set recorded in 1991 in West Texas between the well JTM-A and JTM-C, [3]. We use 100 shots and 100 receivers between depths of 800 m and 950 m. The distance between the wells is 180 m. A shot panel is shown in Figure 9.

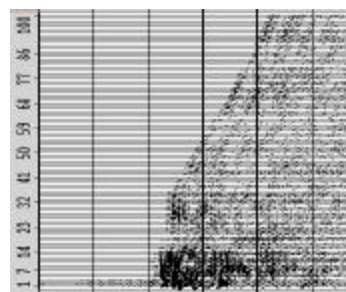


Figure 9: a shot panel of the Mc Elroy data set. The vertical axis represents the receivers and the horizontal axis the time.

As the structure between the two wells is mainly 1D, the velocity model only depends on the depth during the optimization. For this reason, we do not use the sonic logs during the optimization. The final result of the optimization is represented Figure 10.

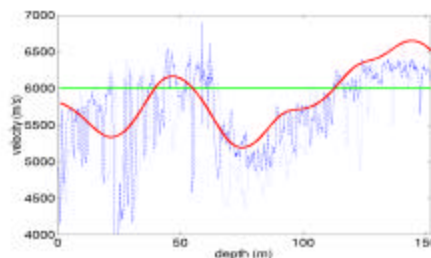


Figure 10: comparison between the optimal velocity model and the sonic logs. The green line represents the initial velocity guess, the red line the optimal velocity model, and the blue lines the sonic logs.

The initial velocity guess was a constant velocity at 6000 m/s. The optimal velocity model agrees with the sonic logs. This result was achieved by manually blanking about 60 % of the data set where multi-valuedness occurs. The optimization took about 1 hour on a workstation.

Automatic crosswell tomography

Real example: Nimir data set

We now apply the technique to a crosswell data set acquired by Petroleum Development Oman [2]. One of the goals is to determine the lateral transition. The sonic logs, shown in Figures 11 and 12, suggest that the top 90 m has a 1D structure whereas the lower 30 m has a 2D structure.

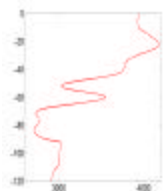


Figure 11: sonic log of the source well

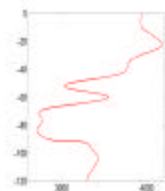


Figure 12: sonic log of the receiver well

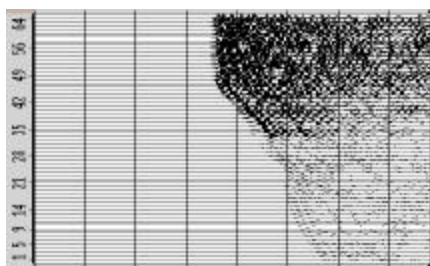


Figure 13: a shot panel of NIMR data set

During the inversion, the velocity model is constrained by the sonic logs. Moreover the velocity model is forced to be 1D in the top 90 m. The initial guess is determined from the sonic logs by interpolation (Figure 14).

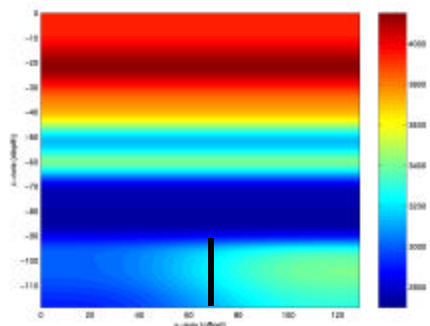


Figure 14: initial velocity guess for the inversion of the NIMR data set. The black line represents the assumed lateral transition.

The final result after optimization is shown Figure 15. The transition can be interpreted as a fault (drawn in black) which is somewhat smoothed. This result agrees with the

result of [2] found with a classical tomography algorithm using picked first-arrival travel-times.

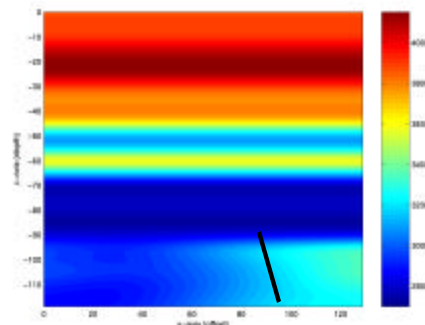


Figure 15: optimal velocity deduced from NIMR data set. The black line represents the interpreted fault.

Conclusions

An automatic crosswell tomography algorithm has been developed based on a semblance and differential semblance optimization. The method avoids the picking of the travel times. However, some pre-processing of the data is required, mainly blanking of the traces where multi-valuedness occurs. Numerical experiments give good results on synthetic and real data, demonstrating the feasibility of this approach.

References

- [1] H. Chauris, M. Noble and P. Podvin, *Testing the behaviour of differential semblance for velocity optimization*, Exp. Abst., EAGE annual Conf, 1998.
- [2] J. Goudswaard, A. ten Kroode, R. Snieder and A. Verdel, *Detection of lateral velocity contrasts by crosswell traveltome tomography*, Geophysics, 63, p. 523-533, 1998.
- [3] J. Harris et al., *High-resolution crosswell imaging of west Texas carbonate reservoir: Part I- Project summary and interpretation*, Geophysics 60, p. 667-681, 1995.
- [4] R.E. Plessix, Y.H. De Roeck and G. Chavent, *Waveform inversion of reflection seismic data for kinematic parameters by local optimization*, SIAM J on Scientific Computing, vol 20 (3), p.1033-1052, 1999.
- [5] W. W. Symes and J.J. Carazzone, *Velocity inversion by differential semblance optimization*, Geophysics, 56, p. 654-663, 1989.
- [6] W.W. Symes, *Inverting waveforms for velocities in the presence of caustics*, TRIP report, 1994.

Acknowledgments

We would like to thank Petroleum Development Oman and Tomoseis for the data sets and Shell International for its permission to publish this paper.